Erratum: Observation of D^0 Meson Nuclear Modifications in Au + Au Collisions at $\sqrt{s_{NN}} = 200$ GeV [Phys. Rev. Lett. 113, 142301 (2014)]

L. Adamczyk, J. K. Adkins, G. Agakishiev, M. M. Aggarwal, Z. Ahammed, I. Alekseev, J. Alford, C. D. Anson, A. Aparin, D. Arkhipkin, E. C. Aschenauer, G. S. Averichev, A. Banerjee, D. R. Beavis, R. Bellwied, A. Bhasin, A. K. Bhati, P. Bhattarai, H. Bichsel, J. Bielcik, J. Bielcikova, L. C. Bland, I. G. Bordyuzhin, W. Borowski, J. Bouchet, A. V. Brandin, S. G. Brovko, S. Bültmann, I. Bunzarov, T. P. Burton, J. Butterworth, H. Caines, M. Calderón de la Barca Sánchez, D. Cebra, R. Cendejas, M. C. Cervantes, P. Chaloupka, Z. Chang, S. Chattopadhyay, H. F. Chen, J. H. Chen, L. Chen, J. Cheng, M. Cherney, A. Chikanian, W. Christie, J. Chwastowski, M. J. M. Codrington, G. Contin, J. G. Cramer, H. J. Crawford, X. Cui, S. Das, A. Davila Leyva, L. C. De Silva, R. R. Debbe, T. G. Dedovich, J. Deng, A. A. Derevschikov, R. Derradi de Souza, S. Dhamija, B. di Ruzza, L. Didenko, C. Dilks, F. Ding, P. Djawotho, X. Dong, J. L. Drachenberg, J. E. Draper, C. M. Du, L. E. Dunkelberger, J. C. Dunlop, L. G. Efimov, J. Engelage, K. S. Engle, G. Eppley, L. Eun, O. Evdokimov, O. Eyser, R. Fatemi, S. Fazio, J. Fedorisin, P. Filip, E. Finch, Y. Fisyak, C. E. Flores, C. A. Gagliardi, D. R. Gangadharan, D. Garand, F. Geurts, A. Gibson, M. Girard, S. Gliske, L. Greiner, D. Grosnick, D. S. Gunarathne, Y. Guo, A. Gupta, S. Gupta, W. Guryn, B. Haag, A. Hamed, L.-X. Han, R. Haque, J. W. Harris, S. Heppelmann, A. Hirsch, G. W. Hoffmann, D. J. Hofman, S. Horvat, B. Huang, H. Z. Huang, X. Huang, P. Huck, T. J. Humanic, G. Igo, W. W. Jacobs, H. Jang, E. G. Judd, S. Kabana, D. Kalinkin, K. Kang, K. Kauder, H. W. Ke, D. Keane, A. Kechechyan, A. Kesich, Z. H. Khan, D. P. Kikola, I. Kisel, A. Kisiel, D. D. Koetke, T. Kollegger, J. Konzer, I. Koralt, L. Kotchenda, A. F. Kraishan, P. Kravtsov, K. Krueger, I. Kulakov, L. Kumar, R. A. Kycia, M. A. C. Lamont, J. M. Landgraf, K. D. Landry, J. Lauret, A. Lebedev, R. Lednicky, J. H. Lee, M. J. LeVine, C. Li, W. Li, X. Li, X. Li, Y. Li, Z. M. Li, M. A. Lisa, F. Liu, T. Ljubicic, W. J. Llope, M. Lomnitz, R. S. Longacre, X. Luo, G. L. Ma, Y. G. Ma, D. M. M. D. Madagodagettige Don, D. P. Mahapatra, R. Majka, S. Margetis, C. Markert, H. Masui, H. S. Matis, D. McDonald, T. S. McShane, N. G. Minaev, S. Mioduszewski, B. Mohanty, M. M. Mondal, D. A. Morozov, M. K. Mustafa, B. K. Nandi, Md. Nasim, T. K. Nayak, J. M. Nelson, G. Nigmatkulov, L. V. Nogach, S. Y. Noh, J. Novak, S. B. Nurushev, G. Odyniec, A. Ogawa, K. Oh, A. Ohlson, V. Okorokov, E. W. Oldag, D. L. Olvitt, Jr., M. Pachr, B. S. Page, S. K. Pal, Y. X. Pan, Y. Pandit, Y. Panebratsev, T. Pawlak, B. Pawlik, H. Pei, C. Perkins, W. Peryt, P. Pile, M. Planinic, J. Pluta, N. Poljak, J. Porter, A. M. Poskanzer, N. K. Pruthi, M. Przybycien, P. R. Pujahari, J. Putschke, H. Qiu, A. Quintero, S. Ramachandran, R. Raniwala, S. Raniwala, R. L. Ray, C. K. Riley, H. G. Ritter, J. B. Roberts, O. V. Rogachevskiy, J. L. Romero, J. F. Ross, A. Roy, L. Ruan, J. Rusnak, O. Rusnakova, N. R. Sahoo, P. K. Sahu, I. Sakrejda, S. Salur, J. Sandweiss, E. Sangaline, A. Sarkar, J. Schambach, R. P. Scharenberg, A. M. Schmah, W. B. Schmidke, N. Schmitz, J. Seger, P. Seyboth, N. Shah, E. Shahaliev, P. V. Shanmuganathan, M. Shao, B. Sharma, W. Q. Shen, S. S. Shi, Q. Y. Shou, E. P. Sichtermann, R. N. Singaraju, M. J. Skoby, D. Smirnov, N. Smirnov, D. Solanki, P. Sorensen, H. M. Spinka, B. Srivastava, T. D. S. Stanislaus, J. R. Stevens, R. Stock, M. Strikhanov, B. Stringfellow, M. Sumbera, X. Sun, X. M. Sun, Y. Sun, Z. Sun, B. Surrow, D. N. Svirida, T. J. M. Symons, M. A. Szelezniak, J. Takahashi, A. H. Tang, Z. Tang, T. Tarnowsky, J. H. Thomas, A. R. Timmins, D. Tlusty, M. Tokarev, S. Trentalange, R. E. Tribble, P. Tribedy, B. A. Trzeciak, O. D. Tsai, J. Turnau, T. Ullrich, D. G. Underwood, G. Van Buren, G. van Nieuwenhuizen, M. Vandenbroucke, J. A. Vanfossen, Jr., R. Varma, G. M. S. Vasconcelos, A. N. Vasiliev, R. Vertesi, F. Videbæk, Y. P. Viyogi, S. Vokal, A. Vossen, M. Wada, F. Wang, G. Wang, H. Wang, J. S. Wang, X. L. Wang, Y. Wang, Y. Wang, G. Webb, J. C. Webb, G. D. Westfall, H. Wieman, S. W. Wissink, R. Witt, Y. F. Wu, Z. Xiao, W. Xie, K. Xin, H. Xu, J. Xu, N. Xu, Q. H. Xu, Y. Xu, Z. Xu, W. Yan, C. Yang, Y. Yang, Y. Yang, Z. Ye, P. Yepes, L. Yi, K. Yip, I.-K. Yoo, N. Yu, Y. Zawisza, H. Zbroszczyk, W. Zha, J. B. Zhang, J. L. Zhang, S. Zhang, X. P. Zhang, Y. Zhang, Z. P. Zhang, F. Zhao, J. Zhao, C. Zhong, X. Zhu, Y. H. Zhu, Y. Zoulkarneeva, and M. Zyzak

(STAR Collaboration)

(Received 24 September 2018; published 28 November 2018)

DOI: 10.1103/PhysRevLett.121.229901

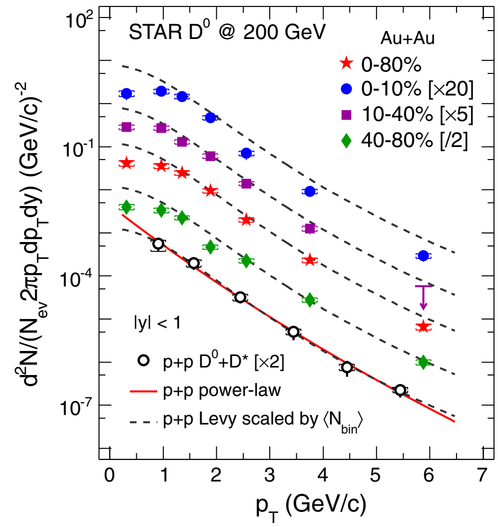

FIG. 2. Centrality dependence of the D^0 p_T differential invariant yield in Au + Au collisions (solid symbols). The curves are number-of-binary-collision-scaled Levy functions from fitting to the $p + p$ result (open circles), which has been updated from Ref. [1] with the latest global analysis of charm fragmentation ratios from Ref. [2] and also taking into account the p_T dependence of the fragmentation ratio between D^0 and $D^{*\pm}$ from PYTHIA 6.4 [3]. The arrow denotes the upper limit with 90% confidence level of the last data point for 10%–40% collisions. The systematic uncertainties are shown as square brackets.

In this Erratum we report changes on the D^0 p_T spectra and nuclear modification factor (R_{AA}) in Au + Au collisions at $\sqrt{s_{NN}} = 200$ GeV by fixing the errors in the efficiency and selection criteria that affected the Au + Au results. The $p + p$ reference spectrum has changed as well and is updated with new fragmentation parameters.

In this Letter, we reported on measurements of the nuclear modification factor of D^0 mesons in Au + Au collisions at $\sqrt{s_{NN}} = 200$ GeV. We have identified two errors in the estimation of the particle identification efficiency. Considering the high combinatorial background in D^0 meson reconstruction in Au + Au collisions, a hybrid particle identification method was used in this analysis to improve significance of the signal. For $p < 1.6$ GeV/c, pion and kaon candidates were selected by requiring a selection on the ionization energy loss of the particle passing through the Time Projection Chamber (TPC), good matching to a hit on the Time of Flight detector (TOF), and a TOF $1/\beta$ (the reciprocal of particle velocity) selection. For $p > 1.6$ GeV/c, candidates were required to pass the TPC ionization energy loss (dE/dx) selection and the $1/\beta$ selection was required for those tracks with good TOF matching. This helps to enhance pion and kaon identification purity. The first error was that in the analysis of the reconstructed data, we did not correctly reject tracks with TOF matching, but with no valid β information due to unavailable calibration parameters. The second error was that we accounted for the efficiency of a distance of closest approach to primary vertex (DCA) selection twice. The DCA-in-the-transverse-plane selection was applied to tracks to insure a good TOF path length calculation by ensuring the tracks are primary. The difference in efficiency from the two errors combined is 30% for single tracks at low p_T and it decreases with increasing p_T compared with the previous result in Au + Au collisions. This results in a factor of 2 higher D^0 yields estimation at $p_T < 2$ GeV/c compared to the case when the correct algorithm is used, affecting results in all centralities in this Letter.

After correcting the two errors, the new D^0 p_T spectra are shown in Fig. 2 as solid symbols for different centrality bins. The vertical bars on the points represent the statistical uncertainties and the brackets denote the systematic uncertainties. The measured D^0 production cross section per nucleon-nucleon-collision at midrapidity in the 0%–10% most-central collisions is updated as $41 \pm 4(\text{stat}) \pm 5(\text{syst})$ μb. The $p + p$ D^0 reference spectrum, shown as open circles, was obtained using the D^0 measurement at $p_T < 2.0$ GeV/c and $D^{*\pm}$ measurement at $p_T > 2.0$ GeV/c. We updated our $p + p$ reference spectrum in this Erratum using the latest global analysis of charm fragmentation ratios from Ref. [2] and also by taking into account the p_T dependence of the fragmentation ratio between D^0 and $D^{*\pm}$ from PYTHIA 6.4 [3], which increases the yield as p_T increases, reaching 40%. The dashed curves are Levy function [4] fits to the $p + p$ reference, scaled by the number of binary collisions, N_{bin} [5]. In our previous $p + p$ collision analysis, TOF matching was always required for the entire p_T region in order to minimize the pileup impact in high luminosity $p + p$ collisions. Therefore, the $p + p$ data were not affected by the error in the Au + Au analysis due to a less complicated algorithm. With these new updates, the $p + p$ D^0 production cross section at midrapidity is measured as $80 \pm 11(\text{stat}) \pm 16(\text{syst})$ μb.

Figure 3 shows D^0 R_{AA} for the centrality bins of 40%–80% (a), 10%–40% (b), and 0%–10% (c). The vertical lines and brackets indicate the statistical and systematic uncertainties, respectively. The vertical bars around unity from left to right

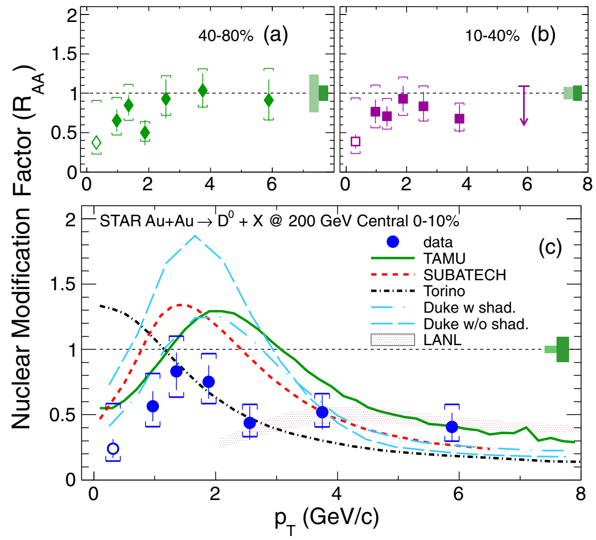

FIG. 3. Panels (a),(b): D^0 R_{AA} for peripheral 40%–80% and semicentral 10%–40% collisions; panel (c): D^0 R_{AA} for 0%–10% most central events (blue circles) compared with model calculations from the TAMU (solid curve), SUBATECH (dashed curve), Torino (dot-dashed curve), Duke (long-dashed and long-dot-dashed curves), and LANL groups (filled band). The open symbol indicates the result with the extrapolated $p+p$ reference. The vertical lines and brackets around the data points denote the statistical and systematic uncertainties, respectively. The vertical bars around unity denote the overall normalization uncertainties in the Au + Au and $p+p$ data, respectively. The R_{AA} probability distribution for the 0–0.7 GeV/c data point is largely skewed. The uncertainty we report is the 68.3% probability range with respect to the measured central value assuming Gaussian distribution.

represent the uncertainties for $N_{\rm bin}$ and the $p+p$ cross section, respectively. The D^0 R_{AA} as a function of p_T is calculated as the ratio between the D^0 yield in each p_T bin for each centrality of Au + Au collisions to the Levy function fit to the $p+p$ data scaled by $N_{\rm bin}$ [1]. The statistical and systematic uncertainties of the $p+p$ reference are displayed in this figure only within the systematic uncertainty of R_{AA}. The uncertainty in the $p+p$ reference dominates this systematic uncertainty, and includes the 1σ uncertainty from the Levy fit and the difference between Levy and power-law function fits for extrapolation to low and high p_T, expressed as 1 standard deviation. The conclusion of strong suppression observed in 0%–10% central collisions for $p_T > 2.5$ GeV/c still holds, while it is consistent with unity in peripheral collisions in this p_T region. At $p_T < 1$ GeV/c, the D^0 yield is found to be suppressed in all centralities. The total charm quark pair yield is expected to follow $N_{\rm bin}$ scaling as charm quarks are believed to be predominately produced in initial hard scatterings. Charm quark hadronization from a coalescence mechanism may lead to an enhancement in the relative fractions of D_s and Λ_c hadrons in heavy-ion collisions [6], therefore resulting in a reduction in the observed D^0 yields in Au + Au collisions. In addition, cold nuclear matter effects, e.g., the nuclear shadowing effect in gluon parton distributions, may also play an important role. In 0%–10% collisions, the suppression level is around 0.5 for $p_T > 3$ GeV/c, which is comparable to both the measurements of electrons from heavy flavor hadron decays [7,8] and the light hadrons [9].

The integrated R_{AA} over p_T is calculated as a ratio of the integrated D^0 yield in Au + Au collisions to that of the $p+p$ reference scaled by the $N_{\rm bin}$ in the given p_T region. Figure 4 shows the integrated D^0 R_{AA} as a function of number of

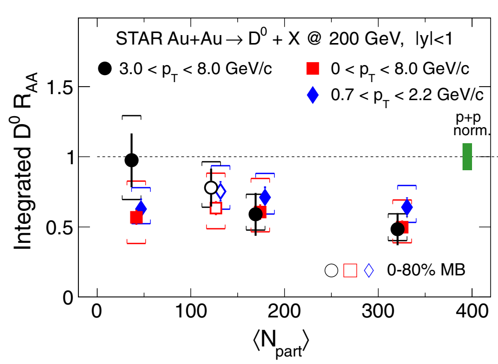

FIG. 4. Integrated D^0 R_{AA} as a function of $N_{\rm part}$ in different p_T regions: 0–8 GeV/c (squares), 0.7–2.2 GeV/c (diamonds), and 3–8 GeV/c (circles). Open symbols are for the 0%–80% minimum bias events. The vertical bar around unity denotes the overall normalization uncertainty from $p+p$ reference.

participants (N_{part}), which represents the collision centrality from the Glauber model [10]. The R_{AA} for $0 < p_T < 8$ GeV/c is suppressed in all centralities and exhibits a weak dependence on N_{part}. The integrated R_{AA} of D^0 is more suppressed at high p_T in more central collisions.

In summary, the original conclusion in the Letter about the suppression of the D^0 R_{AA} at $p_T > 3$ GeV/c is still valid. The bump structure in the intermediate p_T region is still there but no significant enhancement is observed. Since the D^0 cross section is suppressed integrated over all p_T, it is difficult to draw a conclusion on the binary scaling of the total charm production cross section, which requires other charmed hadron measurements.

[1] L. Adamczyk *et al.* (STAR Collaboration), Phys. Rev. D **86**, 072013 (2012).
[2] M. Lisovyi, A. Verbytskyi, and O. Zenaiev, Eur. Phys. J. C **76**, 397 (2016).
[3] T. Sjstrand, S. Mrenna, and P. Skands, Eur. Phys. J. C **0605**, 026 (2006).
[4] C. Tsallis, J. Stat. Phys. **52**, 479 (1988).
[5] B. I. Abelev *et al.* (STAR Collaboration), Phys. Rev. C **79**, 034909 (2009).
[6] M. He, R. J. Fries, and R. Rapp, Phys. Rev. Lett. **110**, 112301 (2013); S. Plumari, V. Minissale, S. K. Das, G. Coci, and V. Greco, Eur. Phys. J. C **78**, 348 (2018); Y. Oh, C. M. Ko, S. H. Lee, and S. Yasui, Phys. Rev. C **79**, 044905 (2009); S. Ghosh, S. K. Das, V. Greco, S. Sarkar, and J.-e Alam, Phys. Rev. D **90**, 054018 (2014).
[7] B. I. Abelev *et al.* (STAR Collaboration), Phys. Rev. Lett. **98**, 192301 (2007).
[8] S. S. Adler *et al.* (PHENIX Collaboration), Phys. Rev. Lett. **96**, 032301 (2006).
[9] B. I. Abelev *et al.* (STAR Collaboration), Phys. Rev. Lett. **97**, 152301 (2006).
[10] P. Shukla, arXiv:nucl-th/0112039.